SIMULTANEOUS MOBILE PM_{10} MONITORING PROVIDES HIGH DEFINITION SPATIAL AND TIME LOCALIZATION OF HOTSPOTS OF POOR AIR QUALITY IN AN URBAN ENVIRONMENT

KAROLINA WALZELOVA[1], SIMON WALZEL[2,*] AND JAN HOVORKA[1]

[1] Institute for Environment Studies, Faculty of Science, Charles University, Prague, Czech Republic
[2] Department of Biomedical Technology, Faculty of Biomedical Engineering, Czech Technical University in Prague, Czech Republic
* Corresponding author: walzesim@fbmi.cvut.cz

ABSTRACT

Many cities suffer from poor air quality resulting from the accumulation of anthropogenic sources of air pollution, especially aerosol particles with an aerodynamic diameter smaller than 10 µm. The urban sources vary significantly in space and time, requiring temporal and spatial monitoring of air quality. Although becoming more common, mobile monitoring still rarely includes a large urban area. The aim was to carry out and analyze a large spatial and temporal monitoring of the variability in air quality in a large urban area in Prague 7. For this purpose, the area of interest was divided into six smaller sub-areas, where a simultaneous and repeated mobile PM_{10} monitoring was done. In the period from December 2019 to May 2020, a total of 174 walks, with a total length of 664 km, were carried out on 10 days. On most of these days, the average PM_{10} concentrations were below the 24-hour limit value (50 µg·m^{-3}), except for one day, which was a critical day for the whole of the city of Prague. The temporal variability in PM_{10} varied significantly with meteorological conditions, independent of location. The spatial variability in PM_{10} revealed that lower concentrations were always recorded in green urban areas and high concentrations in two types of hotspots, non-coincidental (regular traffic, residential heating) and coincidental (heavy vehicles, cigarette smoke). The method of collecting and evaluating the data allowed a high spatial and temporal PM_{10} distribution monitoring and can be used to identify anomalies occurring in urban areas and for other pollutants at different locations.

Keywords: anthropogenic pollution source; hotspots identification; mobile monitoring; PM_{10}; urban air quality

Introduction

Due to the high concentration of anthropogenic sources and restricted airflow high concentrations of airborne particles mostly occur in cities, where they negatively affect a large number of people and the surrounding environment (Gómez-Moreno et al. 2019). In many cities, aerosol particles with an aerodynamic diameter of less than 10 µm, $PM_{10,}$ are the main pollutant of concern, with traffic, industrial activity, construction activity, residential heating and resuspension being the main sources (Meng et al. 2019).

Air pollution with PM_{10}, along with $PM_{2.5}$, nitrogen dioxide (NO_2), ozone (O_3) and benzo(a)pyrene (BaP) are of major concern, primarily because of its adverse effects on human health (EEA 2025). Polluted air is associated with an increased incidence of respiratory, cardiovascular and dermatological diseases, higher incidence of hospital admissions and premature deaths (Cohen et al. 2017). According to the World Health Organization (WHO), 4.2 million people died prematurely due to air pollution in 2016, with 400,000 deaths per year occurring in Europe (WHO 2018a). The total number of "years of life lost" worldwide is 123 million per year (Lelieveld 2017). Of all the pollutants listed, PM_{10} is considered to be the most dangerous and therefore is also a key indicator of air quality (Kobza et al. 2018; WHO 2018b).

In considering the health of urban residents, it is necessary to identify locations that regularly have higher concentrations of air pollutants than their surroundings. In air quality terms, these locations are called "hotspots" (Gómez-Moreno et al. 2019). Urban hotspots are usually located close to their sources. If the position of the source of the pollution does not change over time it is considered to be a non-coincidental source. On the other hand, if the source of the pollution moves and is not associated with one place it is considered to be a coincidental source.

With the majority of the world's population living in cities, it is essential to monitor air quality carefully and to have a good understanding of the main sources of pollution and, therefore, the most important sources. The monitoring of urban air quality is typically done at particular locations (for example, in the Czech Republic, air quality is continuously monitored by a network of stations operated by the Czech Hydrometeorological Institute), but this approach has limitations:

1. Monitoring is done at only a few selected locations. As a result, specific and up-to-date information on air quality may be lacking for particular urban areas. This can be a problem for spatial planning or for the implementation of measures to reduce ambient air pollution. Although dispersion models include these areas, the calculated values can be inaccurate and may not characterize the actual pollution. Furthermore, the use of air pollution models for urban environments is often not appropriate due to the vertical structure of cities and a large number of other factors (Braniš et al. 2009).

Walzelova, K., Walzel, S., Hovorka, J.: Simultaneous mobile PM_{10} monitoring provides high definition spatial and time localization of hotspots of poor air quality in an urban environment
European Journal of Environmental Sciences, Vol. 15, No. 1, pp. 34–42
https://doi.org/10.14712/23361964.2025.5

2. In many cities, monitoring stations are usually located in places where the highest concentration levels of pollution are expected (e.g. along busy streets) (Berkowicz et al. 1996). However, measurements in these environments are strongly affected by local conditions, so values obtained in this way cannot be considered representative of a whole city and should be interpreted with caution, especially when comparing the air quality in different cities or when assessing human exposure to pollution (Berkowicz et al. 1996; Van Poppel et al. 2013).
3. In some cases, stations cannot be located at a site of interest because of its often-large size (covering an area in the order of several square meters), accessibility (e.g., regular inspections, technical repairs, filter changes and sample collection for analysis), and safety rules for operating in a public place (e.g., avoiding electric shocks, not obstructing the view of roads).
4. Data recorded at fixed stations are often only representative of the immediate vicinity and pollutant concentrations may be quite different from those recorded further away. Since it is not possible to build a network of stations that would cover the whole area, dispersion modelling of air pollution is used. Although modelling is very useful, it still does not provide very accurate temporal and local data, as it is based on simplified assumptions of pollutant behaviour (Braniš et al. 2009).

To overcome these limitations, it may be desirable to use mobile measurements (Samad and Vogt 2020). This strategy is based on collecting air pollution data by making real-time measurements in the area of interest using portable devices. Devices can be carried by people or installed on cars, bicycles, etc. However, measurements collected using cars are limited to roadways and cars contribute to air pollution.

Repeated mobile measurements in urban environments provide a fairly accurate picture of the spatial and temporal distribution of pollutants (Van Poppel et al. 2013). For example, Berghmans et al. (2009) measured the exposure of cyclists to ultrafine particles (UFP) in an urban environment using a specially equipped bicycle. Many studies have used mobile stations to quantify the exposure of urban passengers using different modes of transport (Panis et al. 2010; Zuurbier et al. 2010; Okokon et al. 2017). Kaur et al. measured their exposure to CO, UFP and $PM_{2.5}$ in urban areas in London (UK) using mobile volunteers to collect the data (Kaur et al. 2005). Maps of mobile measurements that reveal the spatial variability in air pollution at a high resolution have been used to characterize the contributions of local sources to UFP (Hagler et al. 2010) and monitor PM_{10} air pollution in urban environments (Peters et al. 2013). Liu et al. report a cross-border study that compared PM_{10}, $PM_{2.5}$, PM_1, particle number concentration, and black carbon, using mobile measurements to study pollutants from heating systems in winter in the Czech Republic and Germany (Liu et al. 2020). Another similar study was carried out in the Czech Republic in an urban environment to monitor air pollution from residential heating by Hovorka et al. (2015).

Although mobile measurements are becoming more popular and there are already methods for setting up and processing the data (Peters et al. 2013; Van Poppel et al. 2013; Van den Bossche et al. 2015), it is still difficult to do this for large areas (including all types of local urban environments), especially in cities.

This paper presents a simultaneous and repeated mobile monitoring of PM_{10} carried out in an urban area in Prague, the capital of the Czech Republic, which aimed at obtaining a high spatial and time resolution of PM_{10}, its variability and identification of significant local PM_{10} hotspots.

Methods

A simultaneous and repeated mobile monitoring of PM_{10} concentrations was carried out in the city of Prague in district 7 with an area of 7.14 km² and more than 47 000 residents (ČSÚ 2021). This area was divided into six smaller sub-areas (Fig. 1) with fixed routes for monitoring of approximately equal length (Tab. 1).

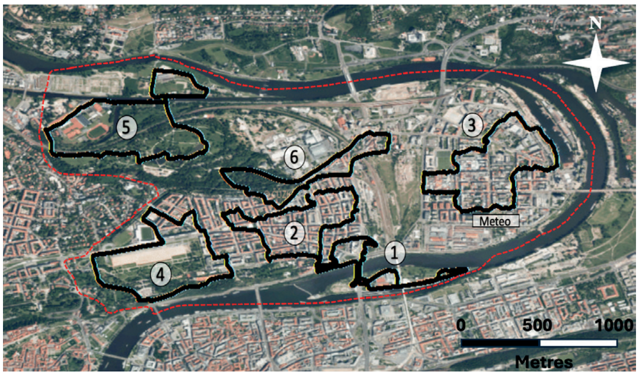

Fig. 1 Map of district 7 in Prague divided into six sub-areas with the routes monitored in black. "Meteo" indicates the location of the WMR 300 meteorological station. The red dashed line marks the borders of Prague 7.

Measurements were made on ten days (weekdays and weekends) between December 2019 and May 2020. Each monitor was assigned a route to measure on a particular day at 08:00, 12:00 and 17:00. The lengths of the routes ranged from 3.4 to 4.5 km.

Equipment

Six DustTrak laser photometers (model 8520, TSI, USA) were used for monitoring PM_{10}. Prior to the start of the monitoring the photometers were calibrated to zero concentrations and airflow measurements done using a factory-calibrated flowmeter. The sampling interval was set to 1 s. To correct for differences between the individual devices, the devices were placed with the sampling heads as close to each other as possible and a joint measurement was made at the Air Quality Laboratory of the Institute for Environmental Studies. Details of the co-location calibration procedure and correction coefficients are provided in the Supplementary Information (Table S1). For the mobile measurements, a photometer was placed in the backpack of each monitor, which sampled air through an omnidirectional sampling head (801565, TSI) that protruded 12–15 cm from the backpack (Fig. 2). Longitude, latitude, altitude, distance from origin and time were recorded by Garmin GPS (models 66s, 64s and eTrex Legend HCx). GPS and DustTrak records were started and stopped simultaneously and paired after each measurement. Meteorological parameters were recorded by Oregon Scientific station (model WMR 300) placed on roofs at a height 24 m above ground (50.101N, 14.451E). Measurements of temperature, air pressure, wind speed and direction, and precipitation were recorded at five-minute intervals.

Table 1 Location and length of the routes in each sub-area.

Route	Sub-area	Length (km)
1	Štvanice Island	3.8
2	Dukelských hrdinů	3.8
3	Holešovice	3.8
4	Letná	3.6
5	Stromovka Forrest Park and Císařský Island	4.5
6	Výstaviště Holešovice	3.4

Fig. 2 Photograph of a DustTrak monitor protruding from the backpack of a member of the monitoring team.

Protocol

Calibration to zero concentration was done prior to each measurement walk. Recording interval, airflow, current time and memory capacity were checked. The completion of all preparatory steps was recorded in the protocol.

During each measurement walk, each monitor filled out their so-called measurement diaries, which were used to document the location of each measurement. In addition to the date, identification number and time of the start and end of the series of measurements, information about events that could significantly affect the accuracy of PM_{10} concentrations (construction, smokers, a passing train, crossing a dusty intersection) were noted along with subjective observations (traffic exhaust, smoke, strong wind swirling dust) and any technical problems with the devices.

Data processing

The data in the internal memory of the DustTrak devices were downloaded using TrakPro software (TSI, USA) and that from the Garmin GPS (models 66, 64s, and eTrex Legend HCx) using BaseCamp software (Garmin, USA). Data processing and analysis, including statistical processing, were done using Microsoft Excel (Microsoft, USA), ArcMap (Esri, USA), CoPlot (CoHort Software, UK) and MATLAB (2020a, Mathworks, USA).

Values less than 1 $\mu g \cdot m^{-3}$ (the detection limit of the DustTrak) were replaced with the detection limit value (1 $\mu g \cdot m^{-3}$) and abnormally high values (above 900 $\mu g \cdot m^{-3}$ and values outside of the PM_{10} rating scale) were removed from the records. The correction coefficients obtained from the co-location calibration procedure were used and urban environment measurements were corrected by multiplying them by 0.32 (Hovorka et al. 2015). This correction was applied because the DustTrak instruments are calibrated for measuring Arizona Road Dust (ISO 12103-1, A1), which differs from typical urban aerosols in particle density, refractive index and size distribution.

Basic statistics were calculated for the PM_{10} data set for each route. The daily and seasonal trend in PM_{10} at each location was tested using the coefficient of divergence (COD). The critical COD value was set at 0.2. Values greater than 0.2 indicate a statistically significant difference between daily measurements (Hovorka et al. 2015). Short-term high PM_{10} concentrations at a location were identified as a hotspot, which were categorized as non-coincidental (traffic, residential heating) and coincidental (cigarette smoke, heavy vehicles) sources. Non-coincidental sources of PM_{10} were defined as those that repeatedly caused an increase in PM_{10} concentrations of at least 1.5 times the median for that particular route and persisted for at least 100 meters. Coincidental sources of PM_{10} were categorized as those that recorded a short-term increase in PM_{10} concentrations and were at least 2 times the median for that route even in units of a few seconds.

Maps with colour-differentiated PM_{10} concentrations

The PM_{10} values recorded by DustTrak combined with the corresponding GPS data and the resulting data file were imported into the ArcMap program of the base map of Prague 7. The points on this map are the PM_{10} concentrations at a given location at a given time and their colour indicates the concentration from dark green (low concentration) through yellow to red (extremely high concentration). This colour scale is the same as the one used for air quality index (AQI) by the US EPA (US EPA 2024), which has been divided into smaller fractions for a more accurate display of data.

Summary 3D graphs with colour-differentiated concentrations of PM_{10}

To compare the profile of PM_{10} concentrations for all routes in a particular sub-area, the PM_{10} values were matched to a sequence of distances unique for each location. A summary 3D graph was then created in CoPlot for each route. The graph shows the trends in PM_{10} at a given time as a function of the distance travelled. The colour-coded values are displayed on a linear scale from 0 to 60 and above in $\mu g \cdot m^{-3}$.

Processing of meteorological data

The meteorological parameters (wind speed and air temperature), recorded at five-minute intervals, were averaged for the days when measurements were recorded and are presented as averages with standard deviations. A wind rose diagram was produced based on the wind speed and direction recorded at the WMR 300 scientific station during the monitoring period. The data were categorized in terms of direction and speed, then the frequency was calculated for each category. The results were then visualized on a polar chart, with the spokes indicating wind direction and their lengths wind speed.

Results

From December 2019 to May 2020, there was a total of 174 monitoring walks over a period of 10 days with a total length of 664 km. Of the ten days, eight were week days and two at weekends, as presented in Table 2. The recorded meteorological parameters (wind speed and air temperature) are presented as averages with standard deviations.

Table 2 Date and day of the week monitored along with the recorded temperatures and wind speeds.

Date	Day of week	Temperature (°C)	Wind speed ($m \cdot s^{-1}$)
09.12.2019	Monday	8.4 ± 1.1	5 ± 1
11.12.2019	Wednesday	0.3 ± 1.9	2 ± 1
20.12.2019	Friday	5.2 ± 3.2	2 ± 1
11.01.2020	Saturday	4.2 ± 1.5	3 ± 1
16.01.2020	Thursday	2.0 ± 2.1	1 ± 1
22.01.2020	Wednesday	0.0 ± 2.9	2 ± 1
06.02.2020	Thursday	0.6 ± 1.5	3 ± 2
20.02.2020	Thursday	4.6 ± 2.0	4 ± 1
22.05.2020	Friday	15.6 ± 3.8	2 ± 1
24.05.2020	Sunday	12.7 ± 2.7	5 ± 2

The average wind speed during the monitoring ranged from 1 to 8 $m \cdot s^{-1}$ and almost half were westerly winds. Southwesterly winds were also common and occurred on one third of the days. The prevailing wind directions at the time of the monitoring are shown graphically in Fig. 3. No precipitation was recorded during the monitoring.

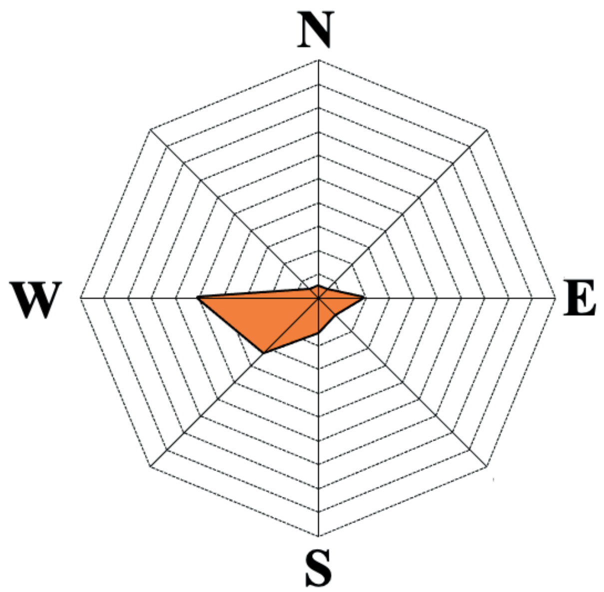

Fig. 3 Windrose for monitoring period.

The effect of seasonal and meteorological conditions on the daily variation in PM_{10}

The 3D graphs with colour-differentiated PM_{10} concentrations in Fig. 4 indicate that highest concentrations were recorded in winter months on weekdays. The concentrations were highest in December and January (median 20 μg·m^{-3}) than in spring (median 4 μg·m^{-3}). At weekends (Saturday, January 11, 2020, and Sunday, May 24, 2020), the concentrations were very low 2–8 μg·m^{-3}. The 3D graphs with colour-differentiated PM_{10} concentrations for five other locations are listed in the Supplementary information.

The highest PM_{10} concentrations were recorded on January 16, 2020, when they were close to the limit value or above the limit value of 50 μg·m^{-3} in the evening. High values were also recorded at the nearby Czech Hydrometeorological Institute on this day, as shown in Table S2. On average, the values in each sub-area were lower than those recorded by the reference station.

A daily trend in PM_{10} was not recorded, except on the most polluted day, January 16, 2020. A table of average PM_{10} values for all the monitoring walks is listed in Supplementary information (Table S3).

Fig. 5 shows all 6 routes monitored simultaneously on a map with colour-differentiated PM_{10} concentrations. The measurements recorded in the evening of January 17, 2020, show a homogeneous distribution of PM_{10} throughout the area in the city sampled. The average concentrations were around 30 μg·m^{-3} both in park areas and more polluted parts. The best day in terms of air cleanliness was May 22, 2020, when the average for Prague 7 was around 4 μg·m^{-3}.

Significantly lower PM_{10} concentrations were regularly recorded in areas of urban greenery compared to other parts of the city. For example, the median PM_{10} detected in Stromovka Forest Park on December 11, 2019, was 4 μg·m^{-3} lower than the median concentration recorded for the rest of the route in this urban environment, as shown in Fig. 6.

Identification of local hotspots and problem areas

During winter several increases in PM_{10} concentrations were recorded at location No. 1 – Štvanice Island, in the vicinity of a refreshment facility located next to a park for skaters, which acted as a local source of air pollution. For example, on December 11, 2019 (Fig. 7),

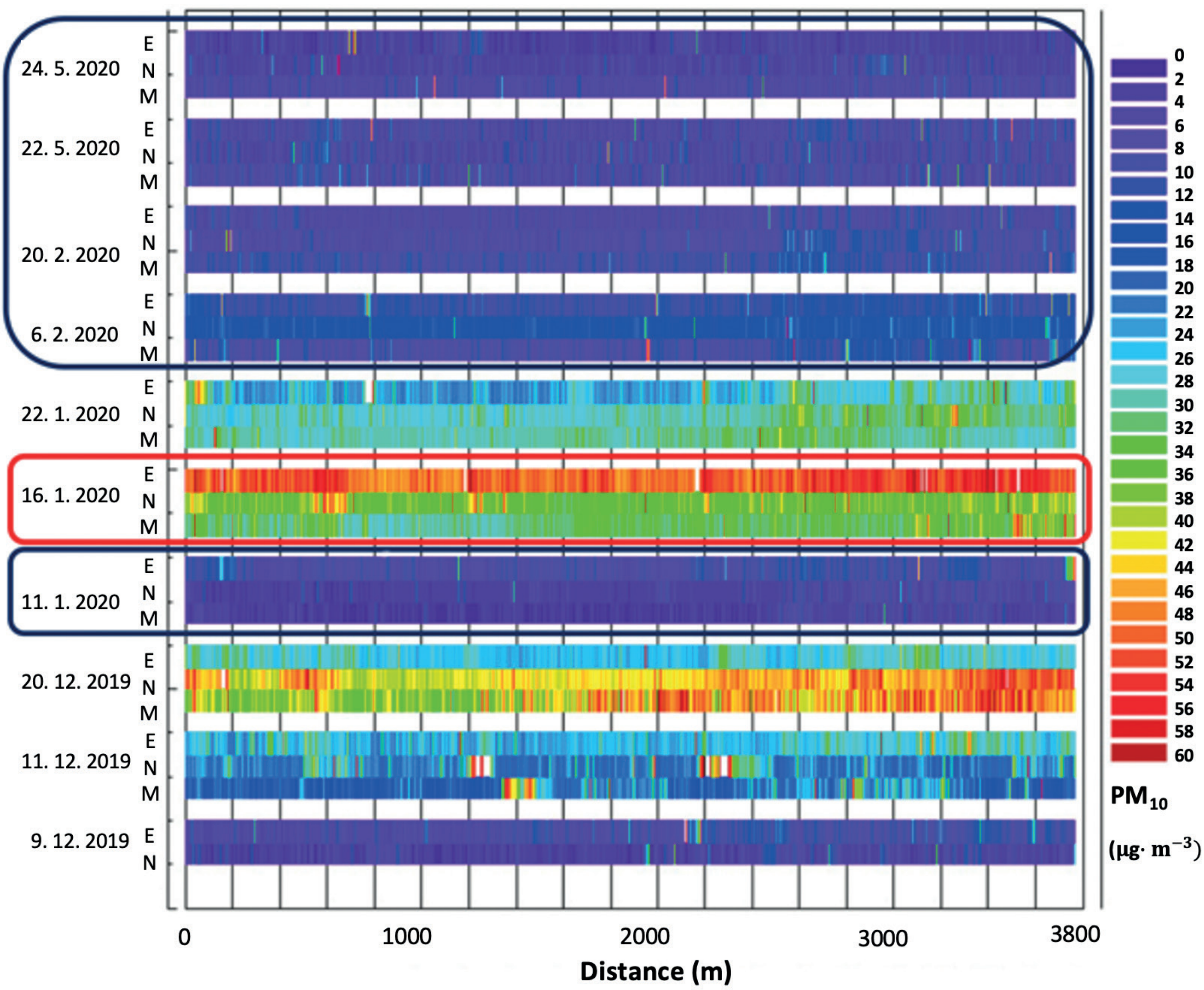

Fig. 4 PM_{10} concentrations on particular days and time of day (M – morning, N – noon, E – evening) depending on the distance travelled during the monitoring walks at location No. 1 – Štvanice Island. Days with very good air quality are indicated along with when the daily limit of 50 μg·m^{-3} for PM_{10} was exceeded on January 16, 2020.

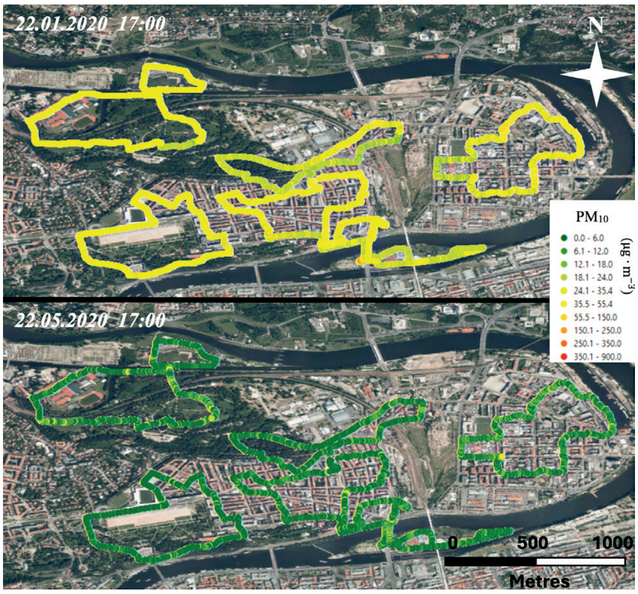

Fig. 5 Aerial photographs showing the level of PM_{10} concentrations recorded along the same monitoring routes in Prague 7 on January 22, 2020, at 17:00 (top) and on May 22, 2020, at 17:00 (bottom).

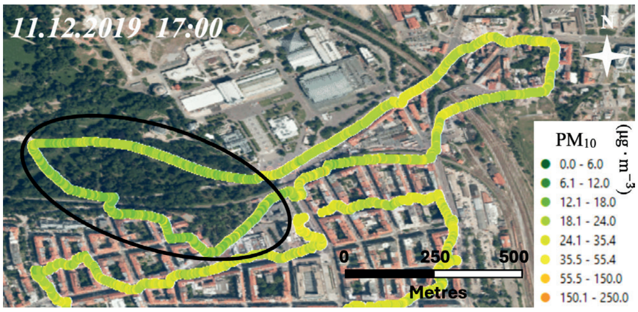

Fig. 6 Aerial photograph showing the effect of urban greenery (area ringed by a black ellipse) on PM_{10} concentrations recorded along a monitoring route.

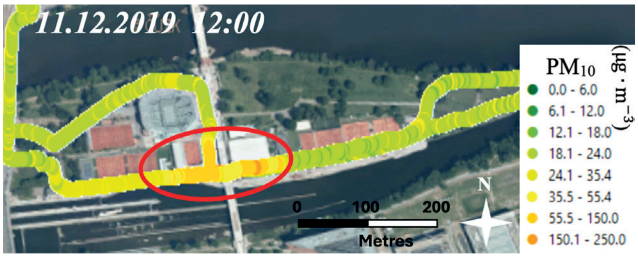

Fig. 7 Aerial photograph showing the 2.8-fold increase in PM_{10} concentrations at location No. 1 – Štvanice Island near a refreshment facility located next to a park for skaters (area ringed by a red ellipse).

the average PM_{10} concentrations were 58 $\mu g{\cdot}m^{-3}$, which was 2.8 times higher than the median concentration for the whole route and the highest value was 180 $\mu g{\cdot}m^{-3}$.

A hotspot was identified at the southern end of Hlávkův bridge. High concentrations of PM_{10} were repeatedly recorded there than at the northern end of the bridge. For example, on January 22, 2020, the concentrations were up to 1.4 times higher at the southern end than at the northern end of the bridge (median PM_{10} at the southern end 29 $\mu g{\cdot}m^{-3}$ and on the northern end 23 $\mu g{\cdot}m^{-3}$).

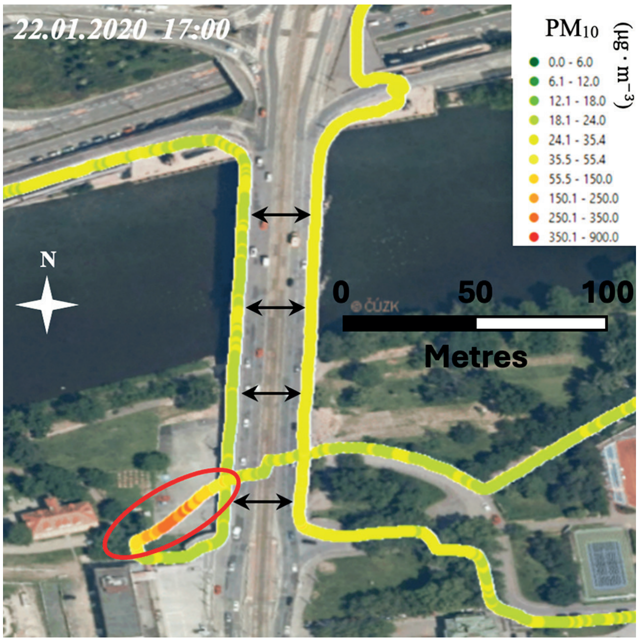

Fig. 8 Aerial photograph of Hlávkův bridge showing the higher concentrations of PM_{10} recorded at the southern end than at the northern end, which is due to the greater level of traffic there (area ringed by a red ellipse) than at the northern end.

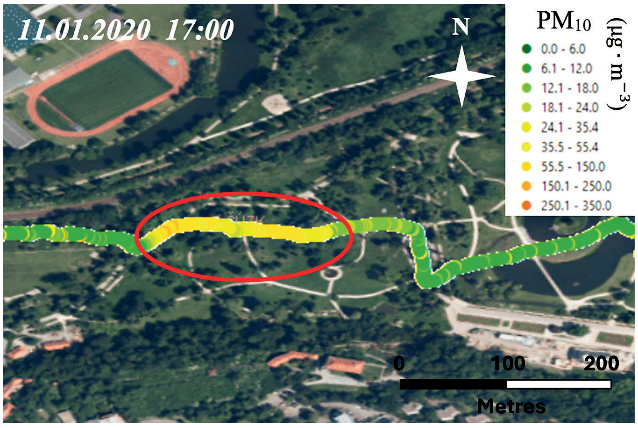

Fig. 9 Aerial photograph showing the location (area ringed by a red ellipse) of the increase in PM_{10} concentrations due to cigarette smokers.

This increase in PM_{10} concentrations was also due to the passage of heavy vehicles and the area affected is ringed by a red ellipse in Fig. 8. The highest value recorded was 300 $\mu g{\cdot}m^{-3}$.

Fig. 9 Map showings the increased PM_{10} concentrations recorded when walking behind smokers. At such locations, PM_{10} concentrations due to cigarette smoke averaged 70 $\mu g{\cdot}m^{-3}$, with the highest concentrations detected 150 $\mu g{\cdot}m^{-3}$.

Discussion

The main finding of this study is a detailed spatial and temporal map of PM_{10} concentrations in an urban area in Prague 7 based on a unique collection of data recorded simultaneously by many mobile monitors.

On most of the days, PM_{10} concentrations in Prague 7 were below the 24-hour limit value (50 μg·m^{-3}) set by the Czech Act No. 201/2012 on the protection of human health. Concentrations above the limit were only recorded on January 16, 2020, which was a critical day for the whole of Prague. This was due to little wind and below average rainfall in that month (ČHMÚ 2020).

The spatial variability in PM_{10} indicate that the concentrations in Prague 7 depend more on the current meteorological conditions than the localities, as the former has a greater influence on the air movement over the area.

In terms of the size of the area of interest, this is a "neighborhood scale" environmental problem (Chow et al. 2002). In order to achieve a more accurate study, the area was divided into six sub-areas where mobile measurements of PM_{10} concentrations were recorded by walking along pre-selected routes, which is suitable for investigating differences at the "microscale" (Chow et al. 2002) or "street level" (Van Poppel et al. 2013). Routes were selected as representative of all types of urban environments including both main roads and less frequented roads, residential areas, public parks and riverside areas and islands in the Vltava River. Particular attention was paid to school facilities, public sports grounds and homes for the elderly, as these are frequented by children, the elderly and physically active people who are then most sensitive to air pollution from a health point of view.

DustTrak devices (model 8520, TSI) were selected because of the following characteristics: their ability to detect mass concentrations of aerosols outdoors in both clean and heavily polluted environments, stability, ease of use, battery operation, intuitive operation, and they can be pre-programmed to record particular parameters. DustTrak devices have been used for similar measurements (Kaur et al. 2007; Peters et al. 2013; Hovorka et al. 2015; Liu et al. 2020). The use of longer sampling heads and putting them in backpacks enabled samples to be collected at the same height as the normal breathing zone of an adult (approximately 150 cm above the ground). To avoid interfering with the sampling zone, team members were instructed not to wear large scarves or have loose long hair and not to smoke during the measurements.

Analysis of the temporal variability in PM_{10} concentrations revealed they were lower in spring (median 4 μg·m^{-3}) than in winter (median 20 μg·m^{-3}) and on weekends than on weekdays. However, remarkably low concentrations of PM_{10} were recorded on January 11, 2020 (median 4 μg·m^{-3}). This was probably because it was a weekend, which compared to the other measurement days in December and January and less likely to be polluted by sources such as traffic, etc. In addition, meteorological conditions may have influenced air quality, as it rained during the night of January 10–11, 2020, which may have washed pollutants out of the air and the moist ground significantly reduced dust and aerosol resuspension the following day.

Very low concentrations of PM_{10} were recorded in February (median 6 μg·m^{-3} on February 20, 2020 and 11 μg·m^{-3} on February 6, 2020). Although the ČHMÚ states that air pollution is usually most severe in February, the graphical yearbook for 2020 reports that the lowest monthly average concentration of PM_{10} was recorded in this month. This is due to the presence of uncharacteristically favourable meteorological conditions in terms of wind above-average temperatures and above-average precipitation, which significantly decreased the concentration of air pollutants (ČHMÚ 2020).

The concentrations recorded on Saturday, January 11, 2020 (median 4 μg·m^{-3}) and Sunday, May 24, 2020 (median 3 μg·m^{-3}) are among the lowest and are likely to be due to the so-called weekend effect in which there is a reduction in emissions of pollutants at weekends and an increase on weekdays. This trend is characteristic of most large cities and occurs in all seasons (Paschalidou and Kassomenos 2004; Elansky et al. 2020). Lower levels of PM_{10} recorded at weekends than on weekdays are also reported by Titos et al. (2014). The reduction of primary emissions at weekends is due to a reduction in human activities (mainly traffic and industry) and is usually even more pronounced on Sundays than on Saturdays (Adame et al. 2014). There were generally no changes in PM_{10} concentrations during the day, but vertical mixing in response to diurnal cycles strongly influenced by sunlight could affect these changes during the day (Sillman 2003).

The maximum concentrations of PM_{10} varied from place to place, as they were directly influenced by specific sources of pollution in the vicinity of the roads. In urban greenery, PM_{10} concentrations were always several units of μg·m^{-3} lower than in city streets. On average, an 18% reduction in PM_{10} concentrations was recorded in urban greenery compared to elsewhere. Thus, greenery can be used as a passive tool for cleaning the air of unwanted pollutants (Gallagher et al. 2015). It is reported that mature trees in urban environments at two sites in England reduced PM_{10} concentrations by 7–26% (McDonald et al. 2007).

Based on the measurements, there are several local hotspots with high PM_{10} concentrations in Prague 7. In all cases they were associated with human activities (traffic, construction work, cigarette smoke or heating). The non-coincidental hotspots included the local heating site on Štvanice Island on route No. 1, the railway crossing in Bubenská street on route No. 6, the construction at Výstaviště in Holešovice on route No. 6 or the southern end of Hlávkův Bridge on route No. 1. As can be seen from the detailed aerial photograph of the island of Štvanice (Fig. 7), there is not only a large tennis court there, but also a skating park, beach volleyball courts and a playground for children. Therefore, the repeatedly recorded high PM_{10} values due to local heating sources in this area are of even more serious concern. In addition, high PM_{10} values, due to construction work, were also recorded at Výstaviště near Jankovského Primary School.

Coincidental sources of PM_{10} were mainly heavy vehicle traffic (e.g., Císařský Island on route No. 5 or Hlávkův Bridge on route No. 1) and cigarette smoke (e.g., Stromovka Forest Park on route No. 5 and Vltavská metro station on route No. 1).

Measures to improve urban air quality should include preventing the emission of dust from construction and demolition sites and of aerosol particles from traffic and local heating, bearing in mind the greater toxic effect of aerosol particles that originate from high-temperature processes. These particles usually include carcinogenic polycyclic aromatic hydrocarbons (Leoni et al. 2016) that are toxic (Topinka et al. 2015) and genotoxic (Topinka et al. 2010) for humans. Therefore, it is advisable to prevent old vehicles from entering the city and to monitor emissions from local heating systems. In order to protect the health of the population, the ban on smoking at public transport stops should also be enforced.

Limitations

This study has several limitations. Although the records spanned a period of six months, they were only collected on ten days. Due to time and financial constraints, it was not possible to continuously measure every day over the course of, say, a year. The monitored days were dependent on the weather and were those, on which there was no rain or snowfall in the area studied and ideally on previous days as well, which wash the pollutants out of the air and thus prevent their detection. Mobile measurements are generally not continuous (e.g. compared to stationary measurements), but episodic. This means that the period of time over which the measurements were recorded was decided prior to the start of the measurements, which are then used to make assumptions about longer time periods. Pollutant concentrations are highly dependent on when they were recorded, however, emission and imission processes in the atmosphere can change rapidly and although it is possible that mobile measurements are good at recording spatial variability, they do not record temporal variability as effectively (Van Poppel et al. 2013).

Conclusion

Simultaneous and repeated mobile monitoring of PM_{10} concentrations was used to describe the spatial and temporal distribution of PM_{10} in Prague 7 and to identify locations with high concentrations of pollution, defined as local hotspots.

In terms of the spatial distribution, PM_{10} concentrations measured over the same time period did not differ significantly between routes, as PM_{10} concentrations depended more on current meteorological conditions than on the location of routes. However, the routes differed in their maxima, the values of which depended on whether the anthropogenic pollution sources were traffic, residential heating or construction.

Concentrations of PM_{10} in Prague 7 were generally below the 24-hour limit value except on one day, which was a critical day for the whole of Prague. Temporal variability revealed lower concentrations at weekends and in spring, as expected, due to reduced human activity and favourable meteorological conditions, respectively.

The results of this study could be used as a basis for decision making on how air quality can be improved and the method used for further studies on the spatial or temporal distribution of several different pollutants.

REFERENCES

Adame J, Hernández-Ceballos M, Sorribas M, Lozano A, De la Morena B (2014) Weekend-weekday effect assessment for O_3, NOx, CO and PM_{10} in Andalusia, Spain (2003–2008). Aer Air Qual Res 14: 1862–1874.

Berghmans P, Bleux N, Panis L, Mishra V, Torfs R, Van Poppel M (2009) Exposure assessment of a cyclist to PM_{10} and ultrafine particles. Sci Total Environ 407: 1286–1298.

Berkowicz R, Palmgren F, Hertel O, Vignati E (1996) Using measurements of air pollution in streets for evaluation of urban air quality – Meterological analysis and model calculations. Sci Total Environ 189: 259–265.

Braniš M, Hůnová I (2009) Atmosféra a klima: aktuální otázky znečištění ovzduší. Praha, Karolinum.

Chow J, Engelbrecht J, Watson J, Wilson W, Frank N, Zhu T (2002) Designing monitoring networks to represent outdoor human exposure. Chemosphere 49: 961–978.

Cohen A, Brauer M, Burnett R, Anderson H, Frostad J, Estep K, Forouzanfar M (2017) Estimates and 25-year trends of the global burden of disease attributable to ambient air pollution: an analysis of data from the Global Burden of Diseases Study 2015. The Lancet 389: 1907–1918.

ČHMÚ (2020) Český hydrometeorologický ústav: Grafická ročenka 2020 [6. 11. 2024]. CHMI.https://www.chmi.cz/files/portal/docs/uoco/isko/grafroc/20groc/gr20cz/Obsah_CZ.html

ČSÚ (2021) Český statistický úřad: Statistický bulletin – Hl. m. Praha – 1. až 3. čtvrtletí 2021 CSU. https://csu.gov.cz/produkty/statisticky-bulletin-hl-m-praha-1-az-3-ctvrtleti-2021.

EEA (2025) European Environment Agency: Air Quality Status report 2025 [9. 4. 2025] EEA Europa. https://www.eea.europa.eu/en/analysis/publications/air-quality-status-report-2025.

Elansky N, Shilkin A, Ponomarev N, Semutnikova E, Zakharova P (2020) Weekly patterns and weekend effects of air pollution in the Moscow megacity. Atmos Environ 224: 117303.

Gallagher J, Baldauf R, Fuller C, Kumar P, Gill L, McNabola A (2015) Passive methods for improving air quality in the built environment: A review of porous and solid barriers. Atmos Environ 120: 61–70.

Gómez-Moreno F, Artíñano B, Ramiro E, Barreiro M, Nuñez L, Coz E, Borge R et al. (2019) Urban vegetation and particle air pollution: Experimental campaigns in a traffic hotspot. Environ Pollut 247: 195–205.

Hagler G, Thoma E, Baldauf R (2010) High-resolution mobile monitoring of carbon monoxide and ultrafine particle concentrations in a near-road environment. J Air Waste Manag Assoc 60: 328–336.

Hovorka J, Pokorná P, Hopke P, Křůmal K, Mikuška P, Píšová M (2015) Wood combustion, a dominant source of winter aerosol in residential district in proximity to a large automobile factory in Central Europe. Atmos Environ 113: 98–107.

Kaur S, Nieuwenhuijsen M, Colvile R (2005) Personal exposure of street canyon intersection users to $PM_{2.5}$, ultrafine particle counts and carbon monoxide in Central London, UK. Atmos Environ 39: 3629–3641.

Kaur S, Nieuwenhuijsen M, Colvile R (2007) Fine particulate matter and carbon monoxide exposure concentrations in urban street transport microenvironments. Atmos Environ 41: 4781–4810.

Kobza J, Geremek M, Dul L (2018) Characteristics of air quality and sources affecting high levels of PM_{10} and $PM_{2.5}$ in Poland, Upper Silesia urban area. Environ Monit Assess 190.

Lelieveld J (2017) Clean air in the Anthropocene. Faraday Discuss 200: 693–703.

Leoni C, Hovorka J, Dočekalová V, Cajthaml T, Marvanová S (2016) Source impact determination using airborne and ground measurements of industrial plumes. Environ Sci Technol 50: 9881–9888.

Liu X, Schnelle-Kreis J, Zhang X, Bendl J, Khedr M, Jakobi G, Zimmermann R (2020) Integration of air pollution data collected by mobile measurement to derive a preliminary spatiotemporal air pollution profile from two neighboring German-Czech border villages. Sci Total Environ 722.

McDonald A, Bealey W, Fowler D, Dragosits U, Skiba U, Smith R, Nemitz E et al (2007) Quantifying the effect of urban tree planting on concentrations and depositions of PM_{10} in two UK conurbations. Atmos Environ 41: 8455–8467.

Meng X, Wu Y, Pan Z, Wang H, Yin G, Zhao H (2019) Seasonal characteristics and particle-size distributions of particulate air pollutants in Urumqi. Int J Environ Res Public Health 16.

Okokon E, Yli-Tuomi T, Turunen A, Taimisto P, Pennanen A, Vouitsis I, Lanki T (2017) Particulates and noise exposure during bicycle, bus and car commuting: A study in three European cities. Environ Res 154: 181–189.

Panis L, de Geus B, Vandenbulcke G, Willems H, Degraeuwe B, Bleux N, Meeusen R (2010) Exposure to particulate matter in traffic: A comparison of cyclists and car passengers. Atmos Environ 44: 2263–2270.

Paschalidou A, Kassomenos P (2004) Comparison of air pollutant concentrations between weekdays and weekends in Athens, Greece for various meteorological conditions. Environ Technol 25: 1241–1255.

Peters J, Theunis J, Van Poppel M, Berghmans P (2013) Monitoring PM_{10} and ultrafine particles in urban environments using mobile measurements. Aerosol Air Qual Res 13: 509–522.

Samad A, Vogt U (2020) Investigation of urban air quality by performing mobile measurements using a bicycle (MOBAIR). Urban Climate 33.

Sillman S (2003) Tropospheric ozone and photochemical smog [Chapter 11]. Sherwood Lollar B, editor. Treatise on geochemistry. Environ Geochem 9.

Titos G, Lyamani H, Pandolfi M, Alastuey A, Alados-Arboledas L (2014) Identification of fine (PM_1) and coarse (PM_{10-1}) sources of particulate matter in an urban environment. Atmos Environ 89: 593–602.

Topinka J, Hovorka J, Milcová A, Schmuczerová J, Kroužek J, Rossner Jr. P, Šrám RJ (2010) Acellular assay to assess genotoxicity of size segregated aerosols. Part I: DNA adducts. Toxicol Lett 198: 304–311.

Topinka J, Rossner Jr. P, Milcova A, Schmuczerova J, Pencikova K, Rossnerova A, Ambroz A, Stolcpartova J, Bendl J, Hovorka J, Machala M (2015) Day-to-day variability of toxic events induced by organic compounds bound to size segregated atmospheric aerosol. Environ Pollut 202: 135–145.

US EPA (2024) United States Environmental Protection Agency: Technical Assistance Document for the Reporting of Daily Air Quality – the Air Quality Index (AQI). AirNow.govhttps://document.airnow.gov/technical-assistance-document-for-the-reporting-of-daily-air-quailty.pdf.

Van den Bossche J, Peters J, Verwaeren J, Botteldooren D, Theunis J, De Baets B (2015) Mobile monitoring for mapping spatial variation in urban air quality: Development and validation of a methodology based on an extensive dataset. Atmos Environ 105: 148–161.

Van Poppel M, Peters J, Bleux N (2013) Methodology for setup and data processing of mobile air quality measurements to assess the spatial variability of concentrations in urban environments. Environ Pollut 183: 224–233.

WHO (2018a) World Health Organization: Ambient (outdoor) air pollution. WHO. https://www.who.int/news-room/fact-sheets/detail/ambient-(outdoor)-air-quality-and-health.

WHO (2018b) World Health Organization: Ambient air pollution: Pollutants.

Zuurbier M, Hoek G, Oldenwening M, Lenters V, Meliefste K, van den Hazel P, Brunekreef B (2010) Commuters' exposure to particulate matter air pollution is affected by mode of transport, fuel type, and route. Environ Health Perspec 118: 783–789.